Journal of Organometallic Chemistry 694 (2009) 2750–2756

Contents lists available at ScienceDirect

Journal of Organometallic Chemistry

journal homepage: www.elsevier.com/locate/jorganchem

Photophysics of Pt(II) 4,6-diphenyl-2,2′-bipyridyl complexes in solution and in LB film

Iswarya Mathew, Wenfang Sun *

Department of Chemistry and Molecular Biology, North Dakota State University, 258 Dunbar Hall, Fargo, ND 58108-6050, United States

ARTICLE INFO

Article history:
Received 6 February 2009
Received in revised form 5 May 2009
Accepted 6 May 2009
Available online 15 May 2009

Keywords:
Square-planar platinum (II) complex
Photophysics
LB film
Electronic absorption
Emission
Transient absorption

ABSTRACT

Two amphiphilic platinum(II) 4,6-diphenyl-2,2′-bipyridyl complexes (**1** and **2**) were synthesized and characterized. LB films of these two complexes were prepared and characterized by AFM technique. Electronic absorption and emission characteristics of these complexes in solutions at room temperature, in glassy solutions at 77 K, and in LB films were studied. The emission energies of the complexes in LB films are similar to those in acetonitrile solutions at room temperature. However, the lifetimes of **1** and **2** in LB films are 4–7 times as long as those in CH_3CN solutions. The triplet transient difference absorption spectra of these complexes exhibit broad absorption in the visible region to the near-IR region. Introducing a hydroxyl substituent on the 4,6-diphenyl-2,2′-bipyridyl ligand favors the formation of intermolecular hydrogen bonding and thus helps the deposition of uniform and stable LB films and increases the self-quenching rate constant for emission of **2** in CH_3CN solution.

1. Introduction

Square-planar Pt(II) complexes have attracted great interests in recent years because of their potential applications as chemical sensors [1], molecular probes for biological macromolecules [2], and in organic light emitting devices [3]. Due to the square-planar configuration of the Pt(II) complexes, intermolecular metal–metal and π–π interactions could occur at high concentration solution or at solid state. For example, a platinum(II) biphenyl dicarbonyl complex was reported to form emissive aggregates in solution at high concentrations [4]. These aggregates are formed due to the weak interactions between the monomers. The energy level of the emissive state was affected by such intermolecular interactions [1b]. Therefore, the emission characteristics of many square-planar platinum complexes largely depend on the extent of molecular aggregation [5]. Although solution phase study of these platinum complexes are crucial and exciting, a significant step towards successful application in various devices would be to prepare and study thin films. It has been reported that solid state emission properties differ remarkably from those shown in solution because of the different degree of metal–metal and π–π interactions [5–7]. However, the emission properties of platinum(II) complex in thin films have not been well understood.

The photophysics of platinum(II) 4,6-diphenyl-2,2′-bipyridyl (dphbph or C^N^N) complexes (Pt(C^N^N)) have been studied extensively by Che and co-workers in solutions [3b,7]. According to their studies, Pt(C^N^N) complexes exhibit stronger emission in comparison to the platinum(II) terpyridyl complexes due to the preferred planar geometry by C^N^N ligand, which reduces the radiationless decay. In addition, it is easier to modify the Pt(C^N^N) complexes by introducing different substituents on the phenyl ring, which would in turn tune the emission property of the complexes. Recently, our group synthesized a series of platinum dphbpy complexes with alkoxyl substituent on the 6-phenyl ring [8]. The introduction of the alkoxyl substituent not only increases the solubility of the complexes in common organic solvents, such as in CH_2Cl_2 and CH_3CN, but also admixes the ^{3}ILCT (intraligand charge-transfer) and $^3\pi,\pi^*$ character with the ^{3}MLCT (metal-to-ligand charge-transfer) character in the emitting state. As a result, the emission quantum yields of these complexes are significantly increased and the excited state lifetimes become much longer. However, the emission of these complexes in solid state has not been studied. In addition, although it has been reported that Pt(II) complexes with alkyl chain can be fabricated as LB films [9], no study on the preparation and investigation of LB films of the Pt(II) dphbpy complexes has been carried out. Because the highly ordered nature of the LB films, the intermolecular interaction in LB films could be different from that in solutions or amorphous solid. The incorporation of the alkoxyl substituent on the phenyl ring of the dphbpy ligand makes these complexes amphiphilic; therefore, it is feasible to prepare LB films of these complexes.

In this work, two amphiphilic platinum dphbpy complexes (**1** and **2** in Fig. 1) were synthesized for the purpose of preparing LB

* Corresponding author.
E-mail address: Wenfang.Sun@ndsu.edu (W. Sun).

0022-328X/$ - see front matter © 2009 Elsevier B.V. All rights reserved.
doi:10.1016/j.jorganchem.2009.05.005

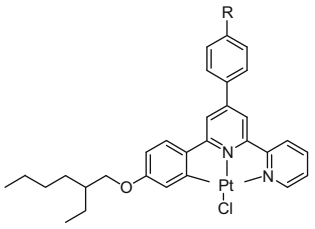

1. R = H; **2**. R = OH

Fig. 1. Chemical structures of **1** and **2**.

films. To evaluate the effect of other intermolecular interactions, such as hydrogen bonding on the preparation and the emission properties of the LB films of the platinum complexes, a hydroxyl group was introduced on the dphbpy ligand for **2**. The photophysical properties of these two complexes in LB films have been systematically investigated. To compare the degree of intermolecular interactions in amorphous solid form to that in LB films, the emission properties of **1** and **2** in amorphous solid form were also investigated.

2. Results and discussions

2.1. Surface pressure–mean molecular area isotherm measurement

Fig. 2 shows the surface pressure–mean molecular area isotherms of **1** and **2** with and without stearic acid (SA) added. The isotherms indicate that the monolayer without SA starts to lift around the same molecular area of *ca.* 60 Å^2 for these two complexes, after which the surface pressure increase sharply. **1** and **2** collapses at a surface pressure of *ca.* 44 mN/m and 58 mN/m, respectively. The observed higher collapse pressure for **2** implies that it forms a more stable film compared to **1**. This could be due to the stabilizing hydrogen bonding formed by the hydroxyl group, which in turn results in expanded monolayer on water. The steepness of the curve for **2** compared to **1** indicates a more likely liquid condensed state for **2**. For the monolayer of **1** mixed with SA, the isotherm starts to lift at a mean molecular area of 90 Å^2. The isotherm collapses at ~54 mN/m.

The limiting molecular areas calculated by extrapolating the plot to zero surface pressure are 46 and 56 Å^2 for pure monolayers of **1** and **2**, respectively, indicating that the molecules take up an "*edge-on*" orientation rather than a "*flat-on*" arrangement [9b] with the alkyl chain sticking out from the air/water interface (illustrated in Fig. 3). The limiting molecular area is found to be ~80 Å^2 for the monolayer of **1** mixed with SA. The estimated molecular areas of **1** and **2**, obtained by geometry optimization through density functional theory (DFT) calculation in vacuum using DMOL^3 program implemented in Material Studio 4.3, are 201 Å^2 (17.8 × 11.3 Å) and 226 Å^2 (17.8 × 12.7 Å), respectively. The tilt angle (θ) (see Fig. 3) with respect to the interface normal can be calculated using the equation sin θ = limiting molecular area/calculated molecular area. The tilt angles thus calculated are 13.2° and 14.3° for **1** and **2**, respectively. The slightly higher limiting area and higher tilt angle of **2** could be due to hydrogen bonding of –OH group with the water subphase, which would allow the (C^N^N)Pt part of **2** to lie more flat on the sub phase compared to **1**.

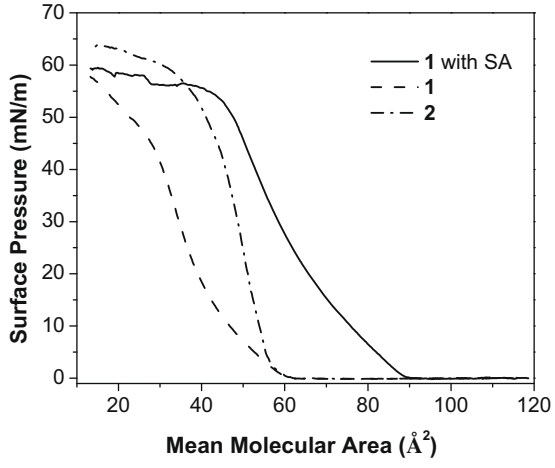

Fig. 2. The surface pressure–mean molecular area isotherms of **1** and **2**.

2.2. AFM images of the LB films

To understand the surface morphology of the LB films, the AFM images of the 5- and 11-layer LB films of **1** and **2** were taken. Fig. 4 shows the AFM height images of the 11-layer films of **1** and **2**. For both complexes, the height images show a uniform grain-like structure. The remarkable difference between the two 11-layer films is that the film for **1** shows larger grain than that for **2**; and the film of **1** is more rough than that of **2**, which is reflected by the brightness of the grain-like structure on each respective film. This phenomenon could be ascribed to the larger aggregates formed in **1** compared to **2**. Due to the presence of intermolecular hydrogen bonding in **2**, each layer deposited could be more uniform and stable compared to that for **1**, which is indicated by the decreased size of the grain-like aggregates. The stabilizing effect of hydrogen bonding in **2** accounts for the well spread film on the subphase, which is then transferred to the glass substrate. The absence of intermolecular hydrogen bonding in **1** results in easier and larger aggregate formation.

2.3. UV–Vis absorption spectra

Fig. 5 shows the UV–Vis spectra of **1** and **2** in acetonitrile solutions and in LB films. In acetonitrile solutions, both **1** and **2** obey Beer–Lambert's law in the concentration range of 1×10^{-6} mol/L to 1×10^{-4} mol/L, indicating that no ground-state aggregation occurs in this concentration range. With reference to the reported platinum terpyridyl or C^N^N complexes [5,6,7c], the absorption bands observed below 400 nm can be assigned to the ligand $^1\pi,\pi^*$ transitions [7c]; while the low-energy absorption band between 400 and 450 nm is ascribed to charge-transfer transitions. According to our previous time-dependent density functional theory (TDDFT) calculation for **1**, the HOMO of **1** is predominantly on the C^N component of the ligand (95.5%), with little contribution (4.5%) from the Pt; whereas the LUMO is dominated by the bipyridine (N^N) component [8]. Therefore, the lowest excited state of **1** is attributed to a mixture of ^{1}ILCT/$^1\pi,\pi^*$/^{1}MLCT. In view of the identical low-energy charge-transfer band of **2** to that of **1**, we believe that **2** has the similar origin of the lowest excited state as that of **1**. In contrast, the molar extinction coefficients and the shape of the $^1\pi,\pi^*$ bands between 250 and 325 nm for **2** are quite different from those of **1**. This could be due to the influence of the –OH group.

In LB films without SA added, with increasing number of layers, the absorbance was found to increase proportionally and the vibronic structures in the UV region disappear. A broad, structureless absorption band appears at *ca.* 300 nm for **1** and 330 nm for **2**, with the tail extended to approximately 525 nm. In contrast, the low-energy charge-transfer band is still clearly evident in the LB film of **1** mixed with SA. Nevertheless, no new absorption band appears at longer wavelength for the LB films, implying that no observable π–π and Pt–Pt interactions occur in the LB films even though the

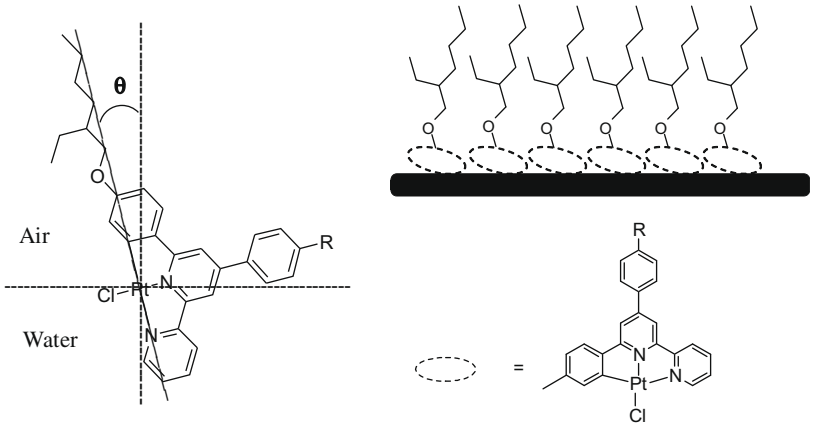

Fig. 3. Proposed molecular orientation and packing at the air-water interface for **1** and **2**.

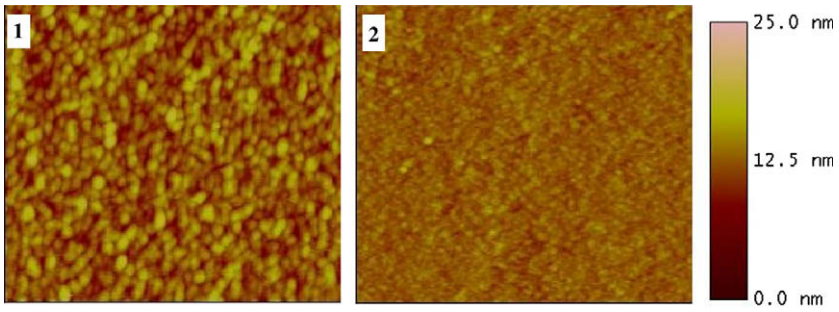

Fig. 4. AFM height images of 11-layer LB films of **1** and **2.** The scan area was 1 μm × 1 μm, and the *Z*-range was 25 nm.

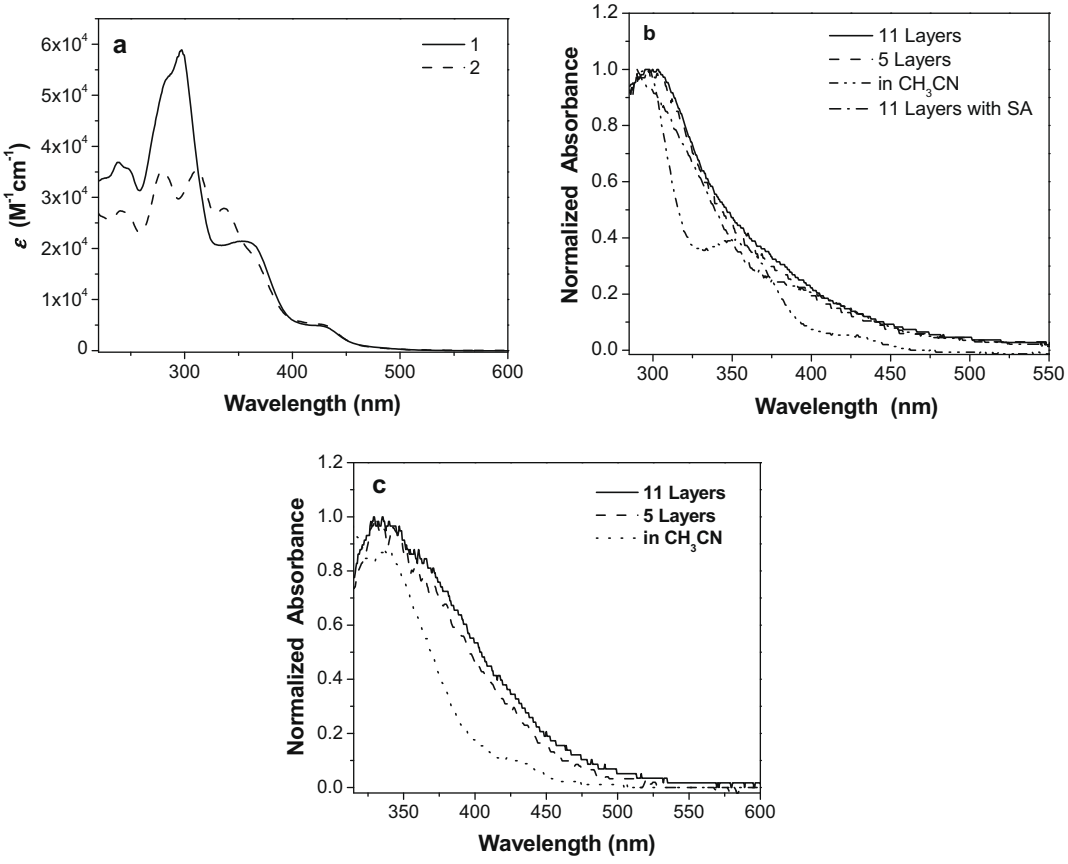

Fig. 5. UV–Vis absorption spectra of **1** and **2** in acetonitrile (a), **1** in LB films (b), and **2** in LB films (c).

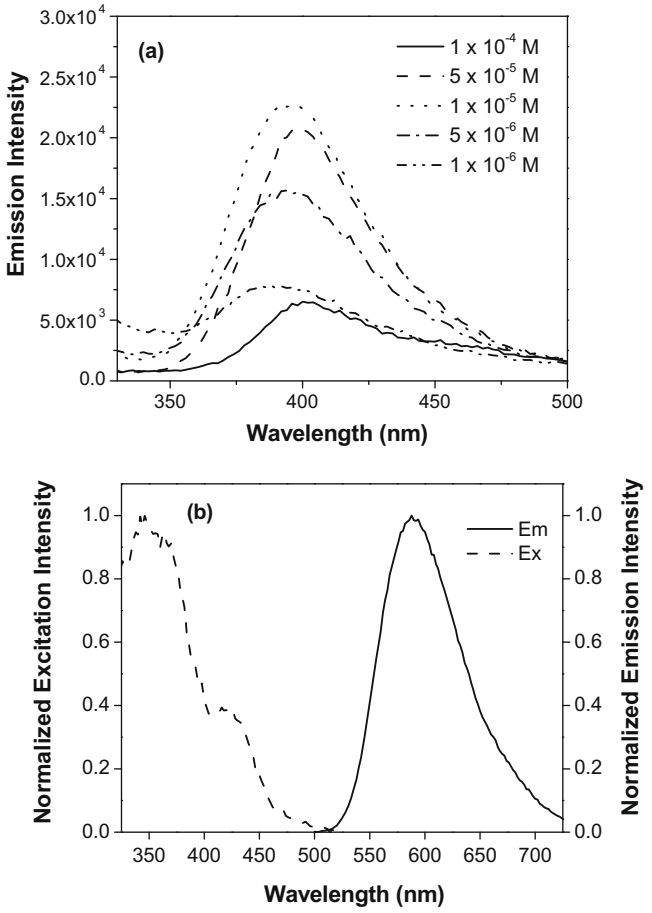

Fig. 6. (a) Concentration-dependent emission spectra of **2** when excited at 279 nm at room temperature. (b) Normalized emission and excitation spectra of **2** at room temperature at a concentration of 1×10^{-5} mol/L in acetonitrile. The excitation wavelength was 420 nm for the emission spectrum measurement, and the excitation spectrum was monitored at λ_{em} = 589 nm.

AFM images indicate some degrees of aggregation. This notion is supported by the similar feature in the visible region of the UV–Vis absorption spectra for the LB films with and without SA mixed. Alternatively, if observable π–π and Pt–Pt interactions present in the LB films without SA, the visible spectral region would be different from that mixed with SA because the dilution from SA would prevent the intermolecular interactions. The absence of intermolecular interactions in LB films is presumably attributed to the "side-on" arrangement of the molecules in the LB films, which is not close enough for the intermolecular interactions to occur.

2.4. Emission studies

Our previous study on **1** revealed that this complex is emissive at r.t. in acetonitrile solution, and the emitting state admixes ^{3}MLCT/^{3}ILCT/$^3\pi,\pi^*$ characters due to the electron-donating effect of the alkoxyl substituent when excited at the low-energy charge-transfer band [8]. Similar to **1**, **2** is also emissive at room temperature in acetonitrile and exhibits dual emission upon excitation at different wavelengths. When excited at the UV region that corresponds to the intraligand $^1\pi,\pi^*$ absorption, *e.g.* 279 nm, **2** exhibits a short-lived (<5 ns) emission band at 395 nm (Fig. 6a). The energy of this emission band coincides with the emission energy of the corresponding C^N^N ligand, thus this emission band is attributed to the $^1\pi,\pi^*$ emission. When the concentration of the solution is increased to 5×10^{-5} mol/L, the emission intensity of this band decreases and the band maximum is red-shifted. Considering the significant absorption at 395 nm, the aforementioned changes of emission at higher concentrations can be attributed to inner-filter effect. In contrast, when excited at the low-energy charge-transfer band, *e.g.* 420 nm, **2** exhibits a broad, structureless emission band at *ca.* 589 nm as shown in Fig. 6b. Compared to its excitation spectrum, the Stokes shift is approximately 170 nm (~7000 cm^{-1}). The intrinsic lifetime of this low-energy emitting state at infinite dilute concentration is deduced to be 625 ns, and the emission quantum yield is approximately 1.2% for this emission band. Considering the large Stokes shift and the long lifetime, we believe that the emission at 589 nm originates from a triplet excited state. In view of the similar structural feature and the same emission energy between **1** and **2**, the emitting state of **2** at 589 nm could also be attributed to a mixture of ^{3}MLCT/^{3}ILCT/$^3\pi,\pi^*$ characters [8,10,11]. The emission intensity of **2** at 589 nm keeps increasing when the concentration increases from 1×10^{-6} mol/L to 1×10^{-4} mol/L, however, the measured lifetimes decrease with the increased concentration. This clearly indicates the occurrence of self-quenching in the concentration range used in our experiment. The self-quenching constant was calculated to be 1.24×10^{10} M^{-1} s^{-1}, which is almost one order of magnitude higher than that measured for **1** in CH_2Cl_2 (Table 1) [8]. This is probably related to the hydroxyl substituent in **2**. The intermolecular hydrogen bonding could favor the formation of excimers, which expedites self-quenching of the excited state.

In acetonitrile glassy solution at 77 K, the emission of **1** and **2** appears at *ca.* 580 nm with a slight shoulder at ~670 nm at a concentration of 1×10^{-4} mol/L when excited at 355 nm. The 0–0 emission is somewhat blue-shifted compared to that at room temperature, with a thermally induced Stokes shift (ΔE_s) of approximately 380 cm^{-1}. Such a small ΔE_s suggest that the emitting state at 77 K could not be a pure charge-transfer state. Considering the similar emission energy at room temperature and at 77 K, we tentatively assign the emitting state at 77 K as ^{3}MLCT/^{3}ILCT/$^3\pi,\pi^*$ as well. The lack of well defined vibronic structure at 77 K is probably due to the poor quality of the CH_3CN glassy solution and the very weak emission. The lifetime measured at *ca.* 580 nm is ~6.4 μs for **1** and **2**, which is the typical lifetime for platinum polypyridine complexes at 77 K [5–7,12]. In contrast, the lifetime monitored at 670 nm is much shorter than that monitored at 580 nm, indicating that the emission at *ca.* 580 nm and 670 nm could originate from different emitting states. With reference to that observed in platinum terpyridyl complexes at 77 K glassy solutions, the lower-energy band could be attributed to the ^{3}MMLCT emis-

Table 1
Emission characteristics of **1** and **2** in CH_3CN solution and in solid forms.

	λ_{em}/nm (τ_0/ns; Φ_{em}; k_Q/M^{-1} s^{-1})		λ_{em}/nm (τ_{em}/μs)	
	In CH_3CN at r.t.	77 K[b]	LB films	Powders
1	590 (460; 0.006; 1.70×10^9)[a]	577 (6.4), 670 (sh., 3.6)	580 (2.1)	583, 622 (sh.)
2	589 (625; 0.012; 1.24×10^{10})	576 (6.3), 670 (sh., 2.8)	580 (4.5)	558 (sh.), 600

[a] From Ref. [8]. The lifetime was measured at a concentration of 2×10^{-5} mol/L. k_Q was measured in CH_2Cl_2 for **1**.
[b] Measured in 1×10^{-4} mol/L CH_3CN glassy solutions. λ_{ex} = 355 nm.

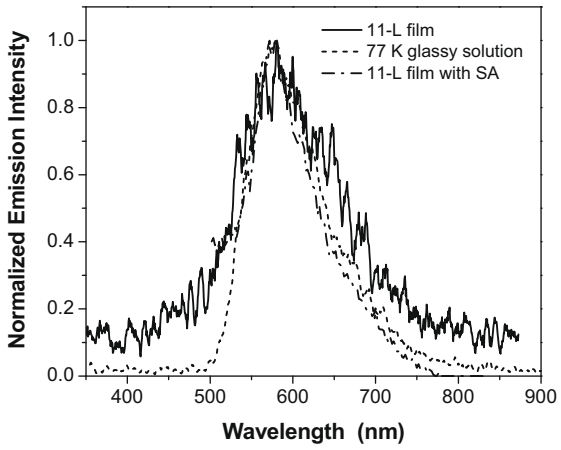

Fig. 7. Emission spectra of **1** in acetonitrile glassy solutions at 77 K and in LB films at room temperature when excited at 355 nm.

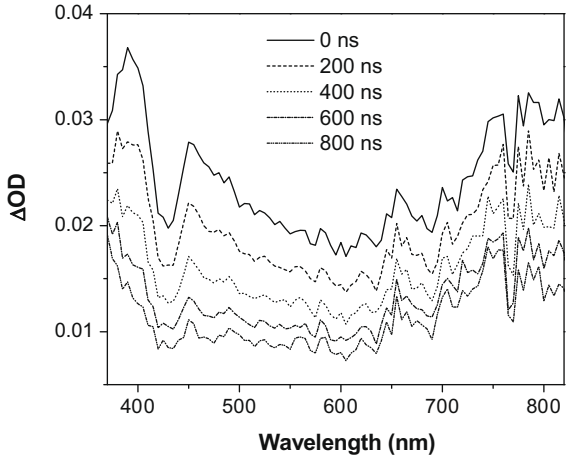

Fig. 9. Time-resolved triplet transient difference absorption of **2** in CH_3CN. The concentration used is 1.8×10^{-5} mol/L. $\lambda_{ex} = 355$ nm. The time indicated in the legend is the delay time after excitation.

sion due to ground-state aggregation at higher concentrations [5a,12]. The occurrence of this band at 77 K but not at room temperature suggests that the association constant for the aggregation could be too small to be observed at room temperature.

Emission was also observed from the LB films and powders of **1** and **2**, respectively, at room temperature. As shown in Fig. 7, emission at *ca.* 580 nm was observed from the LB film of **1**, which appears at the similar energy as those observed in acetonitrile solutions at room temperature and in glassy solution at 77 K. The emission from the 11-layer LB film of **1** mixed with stearic acid also appears at the same energy of 580 nm (shown in Fig. 7). These features clearly indicate that no intermolecular interactions occur in the LB films, which is consistent with the results observed from the UV–Vis absorption study and could be attributed to the '*side-on*' arrangement in the LB film. The same emission energy and feature were observed in the LB film of **2** (see Table 1). In addition, the observed emission lifetimes for the LB films of **1** and **2** are of the order of microseconds, which are comparable to those observed in acetonitrile glassy solutions at 77 K for these two complexes. The elongated lifetimes in LB films compared to those in CH_3CN solutions at room temperature should be attributed to the absence of solvent quenching effect in solid films and to the reduced non-radiative decay rates in solid phase.

Fig. 8 shows the emission spectra of **1** and **2** in solid state as powders. When excited at 430 nm, structured emission spectra with band maxima at 558 nm and 600 nm was observed for **2**. The vibronic spacing is *ca.* 1254 cm^{-1}, corresponding to the aromatic vibration mode of the C^N^N ligand. The same emission feature was observed when excited at 355 nm. When the excitation spectrum was monitored at 560 nm and 600 nm, respectively, identical spectra were observed. This indicates that the two emission bands originate from the same emitting state. The similar phenomenon was observed for **1**, with the dominant emission peak appearing at 583 nm and a shoulder at ~622 nm, and the vibronic spacing being of *ca.* 1075 cm^{-1}. With reference to the similar emission energy to those observed in solution and in LB film at room temperature, and in glassy solution at 77 K, the emitting state of **1** and **2** in amorphous solid (powders) is tentatively assigned to ^{3}MLCT/^{3}ILCT/$^3\pi,\pi^*$ as well. The emission from the amorphous powders is repeatable even when measured at different times.

2.5. Triplet transient difference absorption (TA)

The time-resolved triplet transient difference absorption spectrum of **1** was reported previously by our group in Ref. [8], the spectrum for **2** is presented in Fig. 9. The spectrum exhibits broad positive absorption bands from 370 nm to 810 nm, implying a stronger triplet excited-state absorption than that of the ground-state in this region. The feature of this spectrum resembles that for **1** reported in Ref. [8]. The triplet excited-state lifetime measured from the decay of the transient absorption at 450 nm is

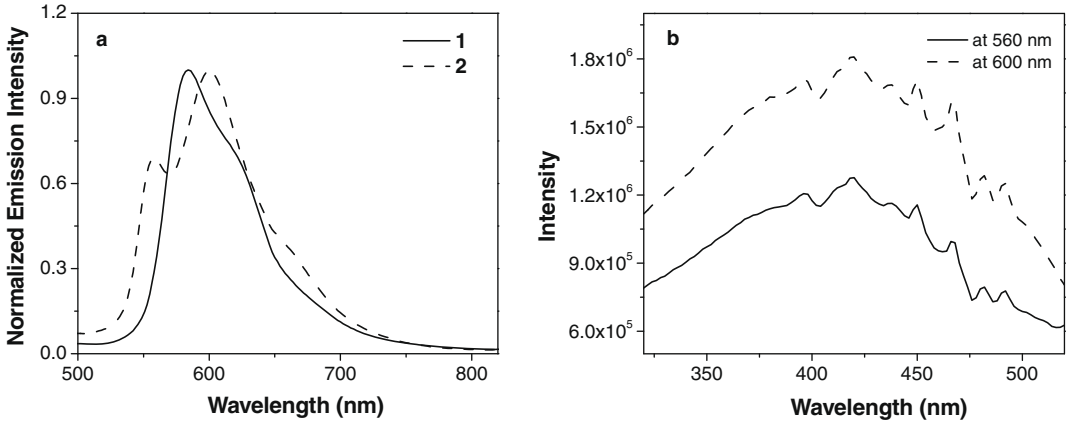

Fig. 8. (a) Normalized emission spectra of **1** and **2** in solid state as powders when excited at 430 nm. (b) Excitation spectra of **2** when monitored at emission wavelength of 560 and 600 nm.

555 ns, which is in line with the lifetime measured from the decay of the emission. This indicates that the transient absorption likely arises from the same excited state that emits or from a state that is in equilibrium with the emitting state. Transient absorption of the LB films could not be measured due to the easy damage of the films upon laser excitation.

3. Conclusion

Emissive LB films are fabricated using amphiphilic platinum(II) 4,6-diphenyl-2,2′-bipyridyl complexes. The emission energy in LB film is similar to that observed in CH_3CN solutions at room temperature; however, the lifetime is much longer in LB film. The emitting state is tentatively attributed to ^{3}MLCT/^{3}ILCT/$^3\pi,\pi^*$. No observable intermolecular interactions are evident in LB films. The presence of the hydroxyl substituent on the C^N^N ligand of **2** could favor the formation of intermolecular hydrogen bonding, which helps the deposition of uniform and stable LB films and increases the self-quenching rate constant for emission of **2** in CH_3CN solution.

4. Experimental

4.1. Synthesis

All the chemicals and solvents were purchased from Aldrich and VWR Scientific Company at analytical grade and used without purification unless otherwise stated. The synthesized products were characterized by ^{1}H NMR (Varian, 400 MHz), and ESI-HRMS (Bruker Daltonics BioTOF III mass spectrometer). Elemental analyses were carried out by NuMega Resonance Laboratories, Inc. in San Diego, California.

The synthesis of **1** has been reported by our group previously [8]. The synthesis of **2** follows a similar synthetic route as illustrated in Scheme 1.

Compound ***3***. In 150 mL acetone, 4′-hydroxyacetophenone (5.44 g, 39.95 mmol), 2-ethylhexyl bromide (8.00 g, 41.42 mmol), potassium carbonate (13.80 g, 99.85 mmol), and catalytical amount of KI were added, and the mixture was refluxed for 36 h. After cooling down, the solution was filtered. Acetone in the filtration was removed and the residue was extracted with dichloromethane. The dichloromethane layer was washed with 50 mL aqueous Na_2CO_3 (10%) and dried with anhydrous Na_2SO_4. Pale yellow oil was obtained as the product (8.80 g, yield: 89%). ^{1}H NMR ($CDCl_3$, 400 MHz) δ: 7.91 (d, J = 8.7 Hz, 2H), 6.91 (d, J = 8.7 Hz, 2H), 3.89 (d, J = 5.7 Hz, 2H), 2.54 (s, 3H), 1.73 (m, 1H), 1.45 (m, 4H), 1.32 (m, 4H), 0.92 (t, J = 7.5 Hz, 6H) ppm.

Compound ***4***. 4-Hydroxybenzaldehyde (1.66 g, 13.59 mmol) was dissolved in 100 mL acetic acid, **3** (3.37 g, 13.58 mmol) and sulfuric acid (98%, 3 mL) were added to the solution. The reaction mixture was stirred at room temperature for 24 h, and then neutralized with 5 M NaOH. The crude product was extracted with ethyl acetate and was purified using column chromatography on silica gel. Ethyl acetate in hexane (v/v = 1/3) was used as the eluent. Pale yellow oil was obtained as the product (3.63 g, yield: 76%). ^{1}H NMR ($CDCl_3$, 400 MHz): δ 8.03 (d, J = 9.3 Hz, 2H), 7.79 (d, J = 15.3 Hz, 1H), 7.54 (d, J = 9 Hz, 2H), 7.43 (d, J = 15.3 Hz, 1H), 6.95 (m, 4H), 3.92 (d, J = 5.7 Hz, 2H), 1.75 (m, 1H), 1.47 (m, 4H), 1.34 (m, 4H), 0.93 (t, J = 7.2 Hz, 6H) ppm.

Compound ***5***. The synthesis of **5** was carried out following the method described in the literature [13]. Yield: 56%. ^{1}H NMR ($CDCl_3$, 400 MHz): δ 8.74 (m, 1H), 8.68 (d, J = 7.8 Hz, 1H), 8.41 (d, J = 1.5 Hz, 1H), 8.13 (d, J = 9 Hz, 2H), 7.91 (td, J = 7.8 & 1.5 Hz, 1H), 7.86 (d, J = 1.5 Hz, 1H), 7.59 (d, J = 8.4 Hz, 2H), 7.39 (m, 1H), 7.04 (d, J = 9.0 Hz, 2H), 6.95 (d, J = 9.0 Hz, 2H), 6.84 (s, 1H), 3.93 (d, J = 6.0 Hz, 2H), 1.77 (m, 1H), 1.47 (m, 4H), 1.36 (m, 4H), 0.95 (t, J = 7.8 Hz, 6H) ppm.

Complex ***2***. Complex **2** was synthesized from **5** according to the reported procedure for similar platinum complex [14]. Yield: 65%. ^{1}H NMR (d_6-DMSO, 500 MHz): δ 8.91 (s,1H), 8.74 (d, J = 7.7 Hz, 1H),

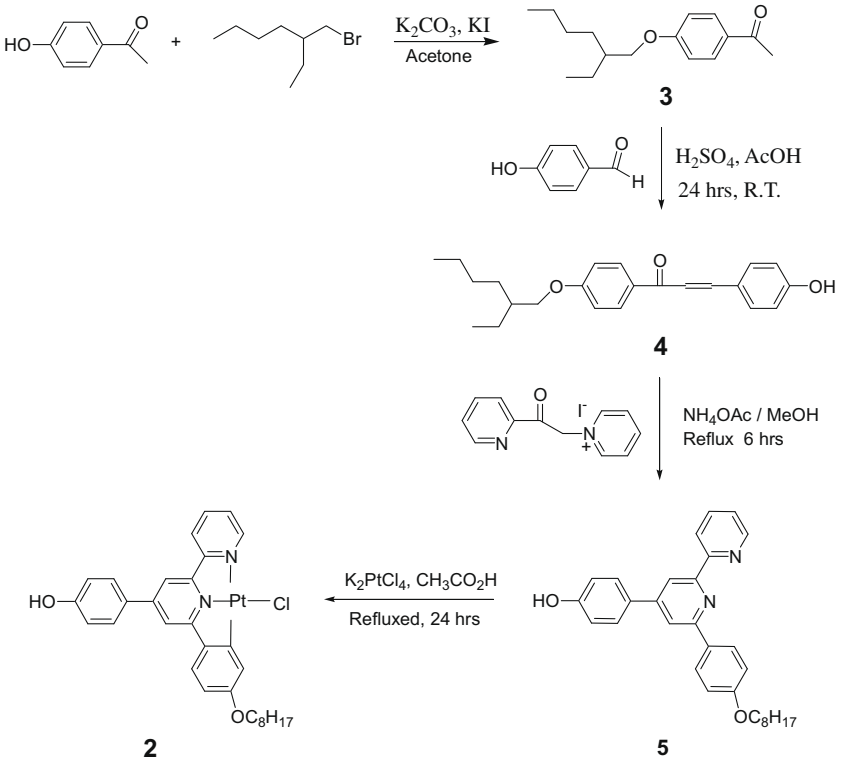

Scheme 1. Synthetic route for complex **2**.

8.37 (s, 2H), 8.09 (s, 1H), 8.02 (d, J = 8.3 Hz, 2H), 7.91 (m, 1H), 7.77 (d, J = 8.5 Hz, 1H), 6.96 (d, J = 8.3 Hz, 3H), 6.68 (d, J = 8.3 Hz, 1H), 3.87 (d, 2H), 1.69 (m, 1H) 1.49–1.32 (m, 8H), 0.95 (t, J = 7.7 Hz, 6H) ppm. ESI-MS m/z calcd for $[C_{30}H_{31}N_2O_2Pt+CH_3CN]^+$: 687.2296. Found: 687.2318 (53%). Anal. Calc. for $C_{30}H_{31}ClN_2O_2Pt$: C, 52.82; H, 4.58; N, 4.11. Found: C, 52.98; H, 4.94; N, 4.11%.

4.2. LB film preparation

Surface pressure–mean molecular area isotherm measurement and LB film preparation were carried out using a KSV minitrough with dimensions of $7.5 \times 30 \times 1$ cm^3. The trough and the barriers were thoroughly cleaned with ethanol and ultra pure water with a resistance of 18 MΩ cm. Wilhelmy method was used to measure the surface pressure. 5 mL solution of **1** in dichloromethane (1 mM) and **2** in 4:1 CH_2Cl_2:CH_3CN was prepared in HPLC grade solvent. Thirty-five microliters solution was spread on ultra pure water subphase at 25 ± 1 °C and was left for 25 min for solvent evaporation. The compression rate was kept at 5 mm/min. All the isotherms were repeated at least three times.

The LB films of **1** and **2** were deposited on hydrophilic glass slides by dipping method. The transfer ratio was near unity for deposition. The glass slides were cleaned and surface pretreated to become hydrophilic before the deposition. This was conducted by cleaning the glass slides by detergent and water, followed by soaking in concentrated H_2SO_4 for 1 h. After which the acid was rinsed and thoroughly cleaned by ultra pure water.

AFM technique was used to study the surface morphology of the film prepared. It was carried out using a Veeco DI-3100 with a silicon nitride probe by tapping mode.

4.3. Spectroscopic studies

UV–Vis absorption spectra were recorded on a Shimadzu 2501 PC UV–Vis spectrophotometer. The steady-state emission spectra in CH_3CN solution and from the amorphous powders at room temperature were measured using a SPEX Fluorolog-3 fluorometer. The emission spectra in LB film at room temperature and in CH_3CN glassy solution at 77 K, the emission lifetime, and the triplet transient difference absorption spectra were obtained on an Edinburgh LP920 laser flash photolysis spectrometer. Excitation source was a Quantel Brilliant Nd:YAG laser with a pulsewidth of 4.1 ns and a repetition rate of 1 Hz. The third-harmonic output (355 nm) from the laser was used as the excitation wavelength.

Acknowledgments

Acknowledgment is made to the USDA-CSREES program (2005-34475-15788 and 2006-34475-17127) and the National Science Foundation (CAREER CHE-0449598) for financial support. We are also grateful to North Dakota State EPSCoR (ND EPSCoR Instrumentation Award) for support. We would like to thank Dr. Hongshan He at the South Dakota State University for helping us to estimate the molecular areas for **1** and **2**.

References

[1] (a) Q.-Z. Yang, ; L.-Z. Wu, H. Zhang, B. Chen, Z.-X. Wu, L.-P. Zhang, Z.-H. Tung, Inorg. Chem. 43 (2004) 5195;
(b) L.Z. Wu, T.C. Cheung, C.-M. Che, K.K. Cheung, M.H.W. Lam, Chem. Commun. 10 (1998) 1127;
(c) K.-H. Wong, M.C.-W. Chan, C.-M. Che, Chem. Eur. J. 5 (1999) 2845;
(d) S.C.F. Kui, S.S.Y. Chui, C.-M. Che, N. Zhu, J. Am. Chem. Soc. 128 (2006) 8297.
[2] D.R. McMillin, J.J. Moore, Coord. Chem. Rev. 229 (2002) 113.
[3] (a) M. Cocchi, V. Fattori, D. Virgili, C. Sabatini, P. Di Marco, M. Maestri, J. Kalinowski, Appl. Phys. Lett. 84 (2004) 1052;
(b) W. Lu, B.X. Mi, M.C.W. Chan, Z. Hui, C.-M. Che, N. Zhu, S.T. Lee, J. Am. Chem. Soc. 126 (2004) 4958;
(c) H. Yesin, D. Donges, W. Humbs, J. Strasser, R. Sitters, M. Glasbeek, Inorg. Chem. 41 (2002) 4915;
(d) A.S. Ionkin, W.J. Marshall, Y. Wang, Organometallics 24 (2005) 619;
(e) J. Brooks, Y. Babayan, S. Lamansky, P.I. Djurovich, I. Tsyba, R. Bau, M.E. Thompson, Inorg. Chem. 41 (2002) 3055;
(f) J.C. Shi, H.Y. Chao, W.F. Fu, S.M. Peng, C.-M. Che, J. Chem. Soc., Dalton Trans. 18 (2000) 3128;
(g) L. Chassot, A. von Zelewsky, D. Sandrini, M. Maestri, V. Balzani, J. Am. Chem. Soc. 108 (1986) 6084;
(h) B.P. Yan, C.C.C. Cheung, S.C.F. Kui, H.F. Xiang, R.S.J. Xu, C.-M. Che, Adv. Mater. 19 (2007) 3599;
(i) W.Y. Wong, Z. He, S.K. So, K.L. Tong, Z. Lin, Organometallics 24 (2005) 4079;
(j) Z. He, W.Y. Wong, X. Yu, H.S. Kwok, Z. Lin, Inorg. Chem. 45 (2006) 10922.
[4] G.Y. Zheng, D.P. Rillema, Inorg. Chem. 37 (1998) 1392.
[5] (a) V.W.W. Yam, R.P.L. Tang, K.M.C. Wong, K.K. Cheung, Organometallics 20 (2001) 4476;
(b) V.W.W. Yam, K.M.C. Wong, N. Zhu, J. Am. Chem. Soc. 124 (2002) 6506.
[6] R. Büchner, J.S. Field, R.J. Haines, L.P. Ledwaba, R. McGuire Jr., D.R. McMillin, O.Q. Munro, Inorg. Chim. Acta 360 (2007) 1633.
[7] (a) C.W. Chan, T.F. Lai, C.-M. Che, S.M. Peng, J. Am. Chem. Soc. 115 (1993) 11245;
(b) T.C. Cheung, K.K. Cheung, S.M. Peng, C.-M. Che, J. Chem. Soc., Dalton Trans. (1996) 1645;
(c) S.W. Lai, M.C.W. Chan, T.C. Cheung, S.M. Peng, C.-M. Che, Inorg. Chem. 38 (1999) 4046;
(d) S.W. Lai, M.C.W. Chan, K.K. Cheung, C.-M. Che, Organometallics 18 (1999) 3327;
(e) W. Lu, M.C.W. Chan, N. Zhu, C.-M. Che, C. Li, Z. Hui, J. Am. Chem. Soc. 126 (2004) 7639;
(f) C.W. Chan, L.K. Cheng, C.-M. Che, Coord. Chem. Rev. 132 (1994) 87.
[8] P. Shao, Y. Li, A. Azenkeng, M. Hoffmann, W. Sun, Inorg. Chem. 48 (2009) 2407.
[9] (a) K. Kobayashi, H. Sato, S. Kishi, M. Kato, S. Ishizaka, N. Kitamura, A. Yamagishi, J. Phys. Chem. B 108 (2004) 18665;
(b) K. Wang, M. Haga, H. Monjushiro, M. Akiba, Y. Sasaki, Inorg. Chem. 39 (2000) 4022;
(c) H. Samha, T. Martinez, M.K. De Armond, Langmuir 8 (1992) 2001;
(d) H. Samha, M.K. De Armond, Coord. Chem. Rev. 111 (1991) 73;
(e) L. Liu, L.-X. Qiao, S.-Z. Liu, D.-M. Cui, C.-M. Zhang, Z.-J. Zhou, Z.-L. Du, W.-Y. Wong, J. Polym. Sci. A: Polym. Chem. 46 (2008) 3193.
[10] S.D. Cummings, R. Eisenberg, J. Am. Chem. Soc. 118 (1996) 1949.
[11] W. Paw, R.J. Lachiocotte, R. Eisenberg, Inorg. Chem. 37 (1998) 4139.
[12] (a) F. Guo, W. Sun, Y. Liu, K. Schanze, Inorg. Chem. 44 (2005) 4055;
(b) V.W.-W. Yam, R.P.-L. Tang, K.M.-C. Wong, X.-X. Lu, K.-K. Cheung, N. Zhu, Chem. Eur. J. 8 (2002) 4066.
[13] F. Kröhnke, Synthesis (1976) 1.
[14] S.C.F. Kui, I.H.T. Sham, C.C.C. Cheung, C.W. Ma, B. Yan, N. Zhu, C.-M. Che, W.F. Fu, Chem. Eur. J. 13 (2007) 417.